

Virtual Laboratory for Technology FES FY2018 Third Quarter Report

Phil Ferguson
for the VLT members



Director's Corner

- Bi-monthly teleconferences are continuing with good representation. Discussion over the last three months has centered on program reviews in preparation for the Committee of Visitors and a fusion prototypic neutron source.
- Preparation for a fusion prototypic neutron source workshop is in full swing. Approximately 30 members of the VLT plan to come together in August to discuss the potential for a near-term, cost-effective neutron source primarily for materials science but with a discussion on other potential uses for the source, including blanket and breeding material, plasma facing components, etc.
- This and future highlights will continue to cover research highlights from recent VLT publications and the main VLT research areas:
 - Magnet Systems; Heating & Current Drive; Plasma Fueling/ ELM Pacing/Disruption Mitigation
 - Plasma Facing Components; Plasma Materials Interactions; Structural Materials
 - Design/Systems studies; Power Handling; Fusion Safety; Fuel Cycle Research; Blanket Technology; Vacuum System

If you have any questions on the information in this report, please don't hesitate to contact us.

Determination of Elliptical Polarization Rotation Direction in ECH Transmission Lines

Scientific Achievement

Low power measurements were done on motorized miter-bend polarizers used for converting the linearly polarized microwave beam from a gyrotron into an arbitrary elliptically polarized beam for Electron Cyclotron Heating in ITER. The polarization rotation direction was then calculated as a function of the settings of the angles of the two polarizers.

Significance and Impact

ECH power, transported through highly oversized corrugated metallic waveguides, must achieve a specific elliptical polarization and rotation direction in order to be launched and absorbed as needed in ITER. These new results greatly expand our confidence in our ability to launch the wave with the desired polarization and the desired rotation direction.

Research Details

The elliptical polarization depends on the angular settings of the two polarizers. The rotation direction is then calculated for each set of polarizer angles.

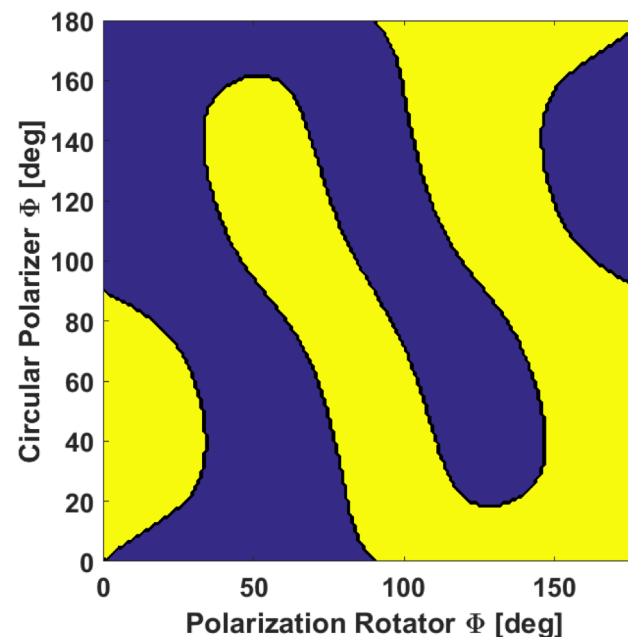
Application

These results are critical to designing the ITER ECH transmission lines but also apply to all other ECH experiments.

MIT: H. Hoffmann, S. Jawla, M. Shapiro and R. Temkin; G. Hanson, ORNL; supported by DOE VLT and US IPO

■ Right-handed

■ Left-handed



Calculated polarization direction (right or left) for the settings of the two miter bend polarizers



U.S. DEPARTMENT OF
ENERGY

Office of
Science



Shattered Pellet Injector Installed on JET for Disruption Mitigation Research in Support of ITER

- JET-SPI is now installed with electrical commissioning to commence in July.
- Cryogenic infrastructure to be installed by JET in August.
- SPI system to be ready for operation in Sept. with experiments now anticipated in December.

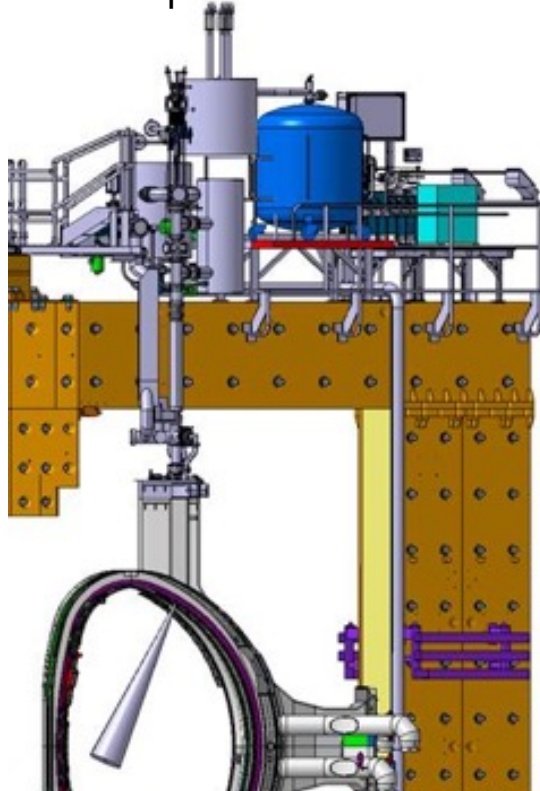
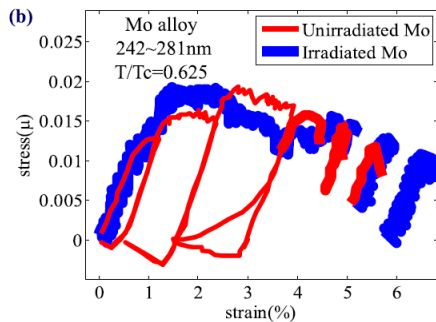
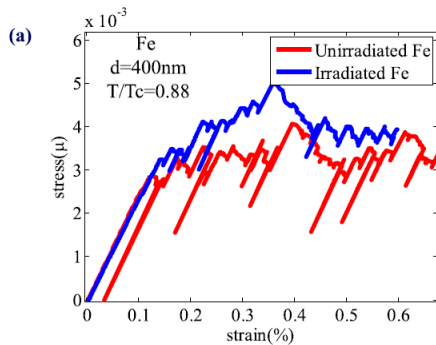


Photo: Top of JET showing SPI mounted vertically

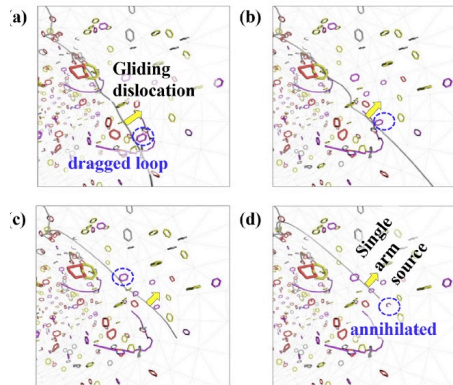
Steve Meitner,
Larry Baylor,
Trey Gebhart

Work sponsored by
DOE Office of Fusion
Energy Sciences

Does Irradiation Enhance or Inhibit Strain Bursts at the Submicron Scale?



(a) Simulation results of a typical stress-strain curve under strain-control, considering the finite machine stiffness effect for unirradiated and irradiated Fe Pillar. (b) Experimental results (see publication below).



Snapshots showing the process of interstitial loop (Burgers vector is $\frac{1}{2}[111]$) dragged by a gliding dislocation line (Burgers vector is $\frac{1}{2}[111]$ gliding plane is (101). The arrow indicates the glide direction of the dislocation line. All loops are initially 5 nm (the apparent size difference is due to 3D rendering).

Scientific Achievement

Metallic structures, when subjected to neutron irradiation, exhibit the phenomenon of “plastic flow localization.” This invariably leads to loss of ductility and embrittlement. Nano-grained materials may offer the potential to suppress this phenomenon .

Significance and Impact

Development of radiation resistant materials requires a solution to the plastic flow localization problem and radiation-induced loss of ductility.

Research Details

Irradiation-induced defects have been experimentally observed either to inhibit or promote strain bursts and lead to plastic flow localization. Through 3D discrete dislocation dynamics simulations, this work unravels the mystery of how and why irradiation-induced defects enhance or inhibit strain bursts in submicron BCC iron and FCC Cu single crystals. It is shown that smaller strain burst amplitudes in irradiated nano- and micro-pillars are obtained under stress control conditions. However, under strain control conditions, bursts are found not to be sensitive to irradiation, despite the arresting effect of radiation defects. This feature is a result of rapid stress relaxation truncating the strain burst, compared with the influence of irradiation-induced defects. In heavily irradiated materials, dislocation avalanches and strain bursts are shown to be promoted.

Yinan Cui*, Giacomo Po, Nasr Ghoniem, “Does irradiation enhance or inhibit strain bursts at the submicron scale?” *Acta Materialia* **132** (2017) 285-297.

Grain Size Variation in Nanocrystalline Silicon Carbide Irradiated at Elevated Temperatures

Science Objective

Nanocrystalline materials have a large volume fraction of grain boundaries that could be efficient sinks for mobile point defects. However, the grains may become more susceptible to irradiation damage at a decreasing size. This study focused on the size variation of SiC nanograins under irradiation at 700 K

Significance and Impact

A size saturation of SiC grains irradiated at 700 K is observed, which shows material resistance to irradiation, a favorable feature for potential applications in nuclear environments

Research Details

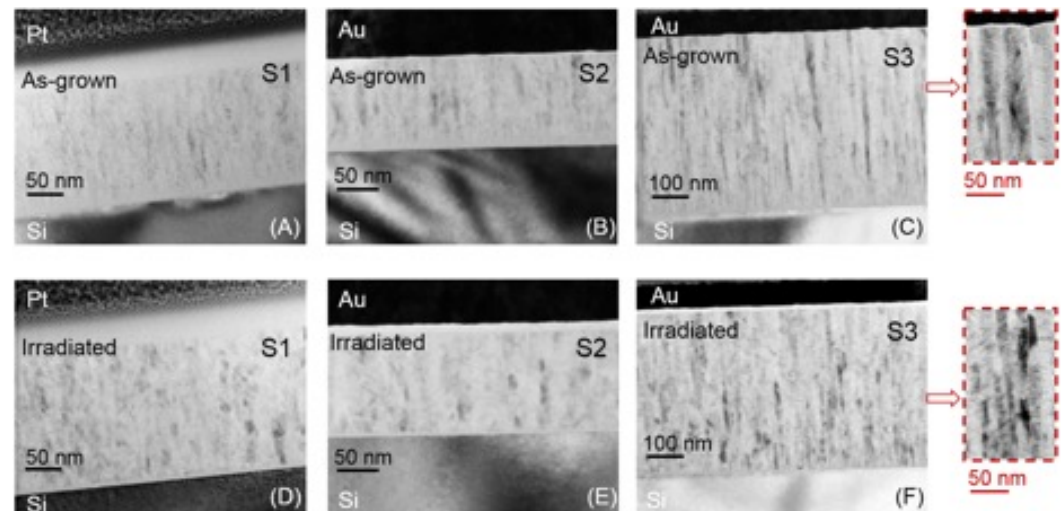
Ion irradiation of nanocrystalline SiC at elevated temperatures leads to growth of small grains that tend to saturate at ~8 nm, while larger grains (~20 nm in size) show a decrease in the size. Homonuclear C-C bonds are found to be graphitized, which may contribute to the size saturation.

L.M. Zhang, W. Jiang *et al.*, *J. Am. Ceram. Soc.* 2018.
DOI: 10.1111/jace.15895

Average grain size and lattice strain determined by GIXRD.

Sample ID	As-grown		Irradiated	
	Size (nm)	Strain (%)	Size (nm)	Strain (%)
S1	2.7 ± 0.5	1.1	5.6 ± 0.8	- 0.07
S2	7.5 ± 1.1	0.92	8.3 ± 1.5	- 0.07
S3	19.7 ± 0.3	0.85	16.8 ± 0.4	0.41

Irradiation leads to lattice relaxation. The larger the grain size, the less the irradiation-induced grain growth. When the grain size exceeds a certain threshold, grain shrinkage occurs due to damage production. Raman data shows C-C bonds are graphitized in SiC during irradiation.



TEM images of nanocrystalline SiC before and after irradiation with 5 MeV Xe ions to 1.15×10^{16} Xe/cm² at 700 K. The SiC grains in sample S3 exhibit a distinct columnar structure that contains a high density of planar defects. The columnar growth of the SiC grains is along the <111> direction.

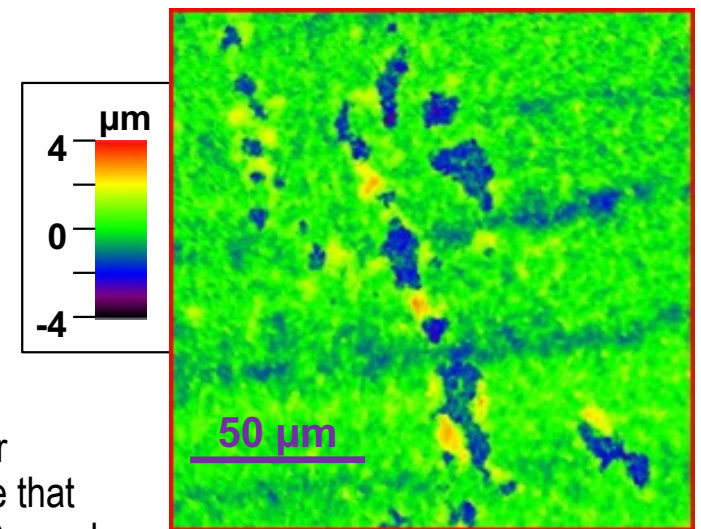
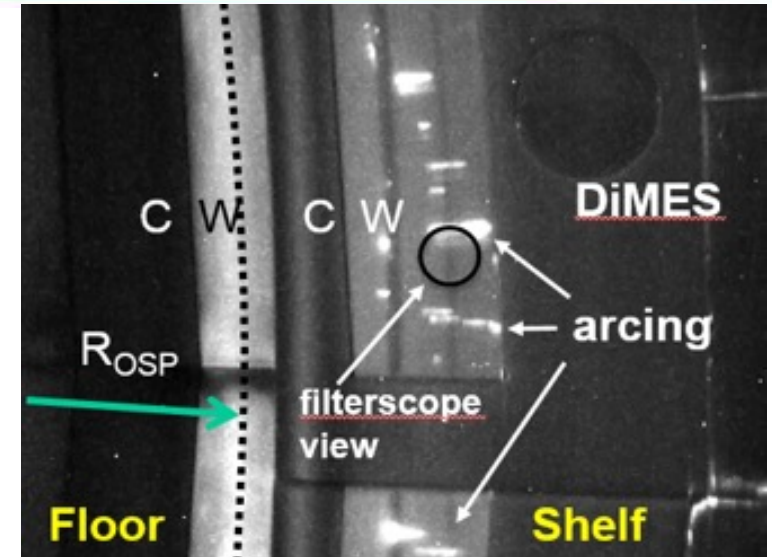
Unipolar arcing causes significant erosion of W PFC surfaces

Scientific Achievement

Unipolar arcing was observed in-situ by optical imaging and spectroscopic diagnostics in DIII-D divertor during Metal Rings Campaign (MRC). Post-mortem tile analysis showed that the amount of W eroded from the shelf tile coatings by arcing was comparable to the total amount of W redeposited in the divertor.

Research Details

- Two almost complete toroidal rings of W-coated TZM tile inserts were installed in the lower divertor of DIII-D for MRC
- With WI-filtered camera arcing was only observed during ELMs, most often on the shelf W insert, over 10 times less often on divertor floor
- Arcing on shelf insert was detected by filterscopes during VDE disruptions
- Post-mortem tile analysis shows arc pits $\sim 2 \mu\text{m}$ deep
- With $\sim 4\%$ of the shelf tile area covered by arc pits, the total amount of W eroded by arcing was estimated at 0.31 g or 1×10^{21} W atoms
- Total amount of W redeposited outside of W rings, from in-vessel XRF measurements, was $1.8 \pm 0.7 \times 10^{21}$ atoms [C. Chrobak, APS/DPP 2016]



Close-up view of an arc trace

Significance and Impact

Tungsten will be used in ITER divertor and is a leading candidate PFC material for devices beyond ITER. Our results confirm previous findings from ASDEX Upgrade that unipolar arcing can be an important erosion mechanism for machines with W PFCs, and should therefore be studied in more detail.

I. Bykov et al., *Phys. Scripta* **T110** (2017) 014034, D. Rudakov et al., PSI-24 Conference (2018)

Softening due to Grain Boundary Defect Formation in Helium Ion Implanted Nanocrystalline Tungsten

Scientific Achievement

The complex damage state of He implanted nanocrystalline W produced a confluence of mechanisms placing softening due to grain boundary defects in competition with hardening from intragranular loop damage.

Significance and Impact

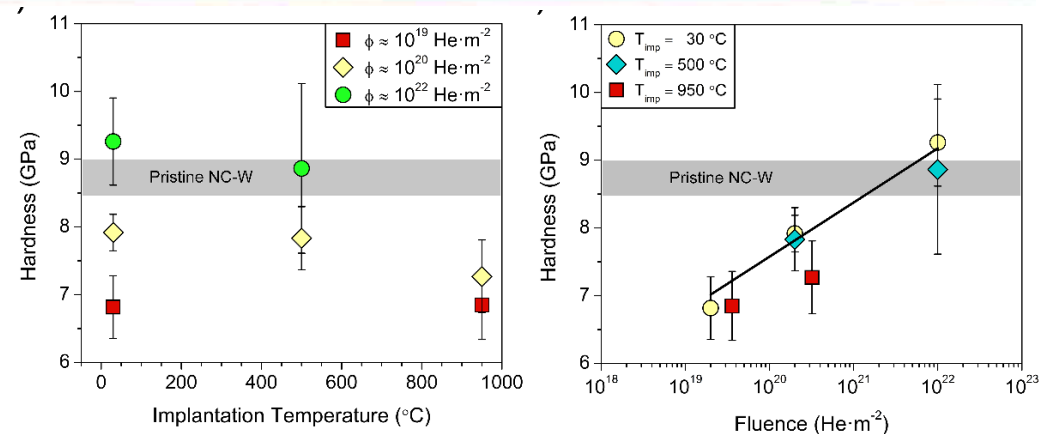
An understanding of competing mechanisms due to coupled defect states will foster new innovations for combating mechanical property degradation from irradiation damage.

Research Details

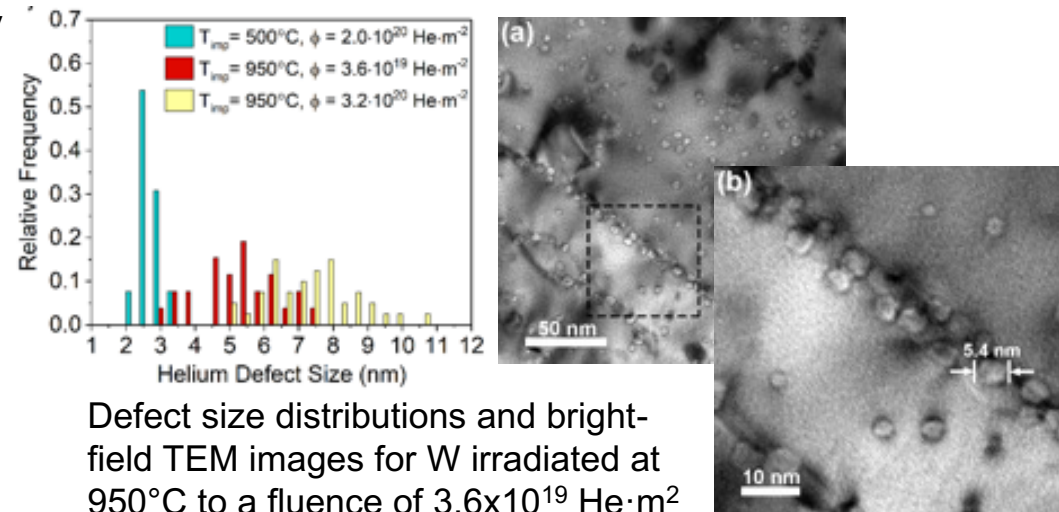
Nanoindentation and TEM experiments were performed on He ion irradiated nanocrystalline tungsten to explore coupled radiation effects and mechanical properties.

Application

These materials have the potential to address stability issues in coarse-grained tungsten for plasma-facing components.



Hardness measurements on He implanted nanocrystalline W



Defect size distributions and bright-field TEM images for W irradiated at 950°C to a fluence of $3.6\cdot 10^{19} \text{ He}\cdot\text{m}^{-2}$

Cunningham, W.S., Gentile, J.M., El-Atwani, O, Taylor, C.N., Efe, M., Maloy, S.A., and Trelewicz, J.R., "Softening due to Grain Boundary Cavity Formation and its Competition with Hardening in Helium Implanted Nanocrystalline Tungsten", Scientific Reports, 8, 2897, 2018

Work sponsored by
DOE Office of Fusion
Energy Sciences

Advanced Materials Modeling Used to Understand/ Improve Tungsten Recrystallization Limits

Science Objective

Here we use molecular dynamics and multiscale modeling techniques in collaboration with the Marian group at UCLA to develop a predictive model of tungsten recrystallization.

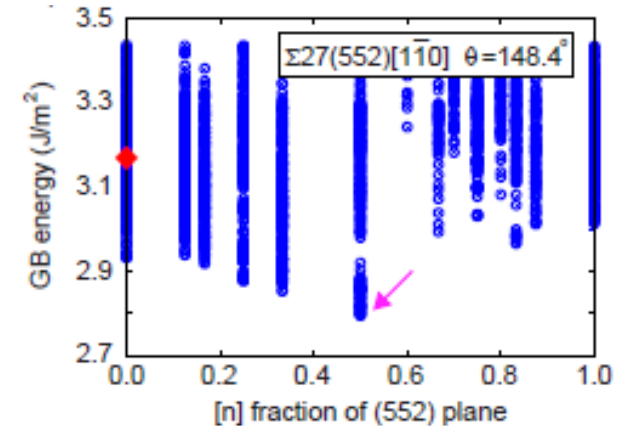
Achievement

We predicted for the first time phase transformations in tungsten grain boundaries (GB) at high temperature. This quarter we have broadened the search to additional grain boundaries in tungsten. In some cases the conventional structure has the lowest energy, but in most cases we found a new ground state.

Why it Matters

Recrystallization limits the operating temperature for tungsten and tungsten alloys in plasma facing components in tokamaks. Recrystallization involves the movement of grain boundaries in damaged metals at high temperature. It is crucial that calculations of GB properties that affect recrystallization start with the correct GB structure, something that has not been possible previously.

New Grain Boundary Structure



An evolutionary algorithm was applied to find new grain boundary structures in tungsten. Each energy point in the plot above corresponds to a different grain boundary structure. The conventional structure is marked with the red diamond. The new ground state at $[n]=0.5$ has a substantially lower energy.

“Grain boundary phases in bcc metals,” T. Frolov et al., *Nanoscale* 10, 8253 (2018);

“Structures and transitions in bcc tungsten grain boundaries and their role absorption of point defects,” T. Frolov et al, submitted *Acta Mater*

Developed and Demonstrated Laser-Based Techniques for Measuring Depth-Dependent He & H concentration in W

Scientific Achievement

Measuring the depth dependence of implanted gas in tungsten divertor and PFC materials is critically important to assess tritium retention anticipated in the ITER divertor & PFCs

Significance and Impact

Tritium retention in tungsten divertor important for establishing ITER tritium inventory

Research Details

Laser-based ablation coupled to in-vacuum Laser Induced Breakdown Spectroscopy (LIBS) using ORNL-developed filterscopes and a quadrupole mass spectrometer to simultaneously perform Laser Ablation Mass Spectrometry (LAMS)

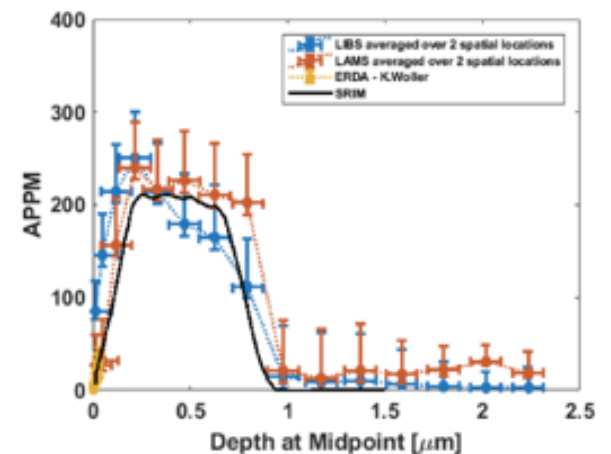
Application

Initial proof-of-principle measurement (using variable energy He-implanted Tungsten) validates LIBS and LAMS technique, and in good agreement with ERDA

Ongoing measurements of plasma-exposed tungsten



532 nm, 5 ns, variable energy Laser ablation added to UTK-ORNL thermal desorption vacuum system

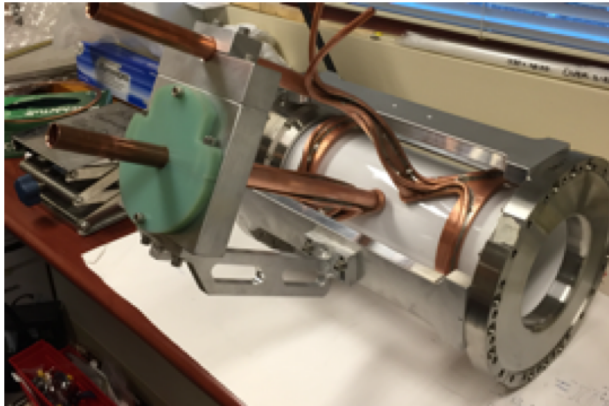


Benchmark experiment demonstrates ability to measure ion-implanted He depth below W by LIBS (orange), LAMS (blue) compared to Elastic Recoil Detection Analysis (yellow) & expected (black line)

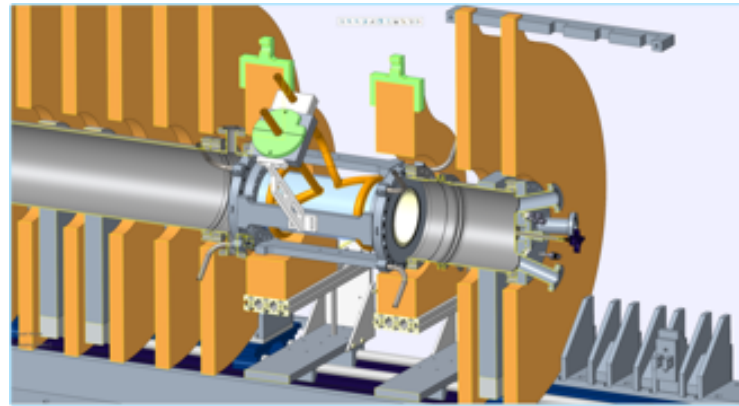
UTK: G. Shaw and B.D. Wirth, ORNL: X. Hu, MIT: K. Woller; supported by DOE Fusion Energy Sciences Fusion Materials Program

UCSD-ORNL RF source technology development for MPEX

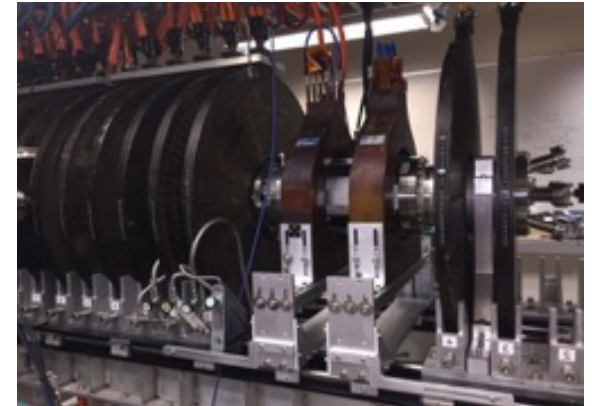
Test Article at UCSD



Rendering on UCSD CSDX Device



Test Article Installed on UCSD CSDX Device



- A high-power water-cooled steady-state RF plasma source has been designed and fabricated by UCSD and ORNL
- The source has successfully generated high-density helicon plasma in CSDX
- The RF source is dimensionally identical to the proposed MPEX plasma source design
- The CSDX source will initially be used for a series of engineering tests to confirm the viability of the higher-power MPEX source design
- Subsequent physics studies in CSDX will investigate material migration and transport, and the evolution of the start-up plasma into a steady-state operational mode

High-Conductivity Graphitic Foam as Plasma-Facing Material

Scientific Achievement

Heat flux and plasma exposure tests with graphitic foam thermal conductivities of 287 W/mK, making it a new plasma-facing material (PFM) candidate in fusion reactors.

Significance and Impact

Graphitic foam has the thermal conductivity of copper at room temperature, but does not melt. It is light weight, easily machined, and has mechanical properties like those of carbon fiber composites (CFC), at much lower cost.

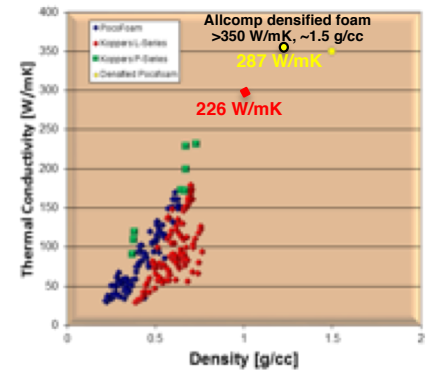
Research Details

Graphitic foam monoblocks press-fit (no braze) to CuCrZr cooling tubes withstood 8 MW/m² fluxes in the GLADIS facility (IPP-Garching). Plasma exposure of foam in the W7-X stellarator (IPP-Greifswald) and PSI-2 facility (KfZ-Jülich) show very low erosion and deuterium retention. W-coated foam substrates are under development.

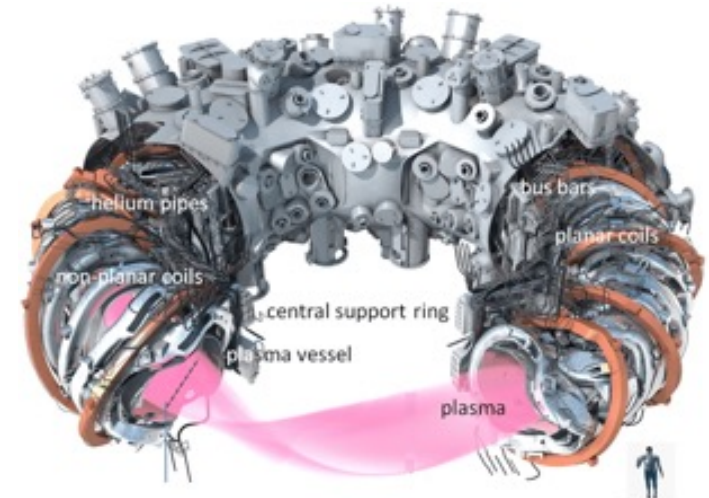
Potential Application

Use for plasma-facing components (PFCs) in W7-X, DIII-D, and WEST.

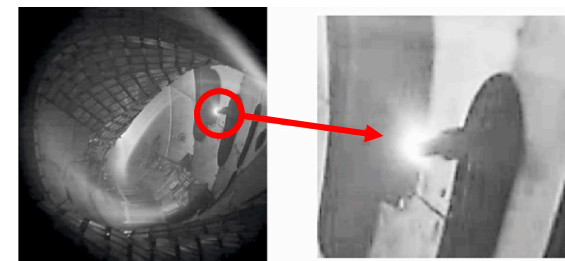
ORNL: D. Youchison, A. Lumsdaine, J. Klett



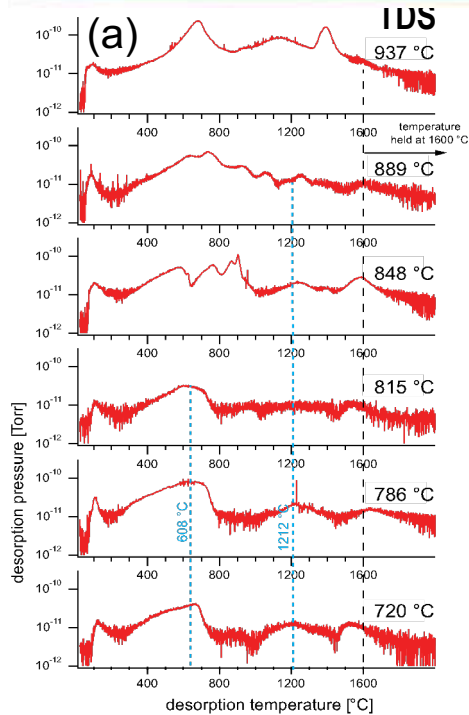
W7-X
Stellarator,
Greifswald,
Germany



Plasma
exposure
in W7-X



Multi-technique analysis of early-stage W nanostructure growth during He plasma exposure



Scientific Achievement

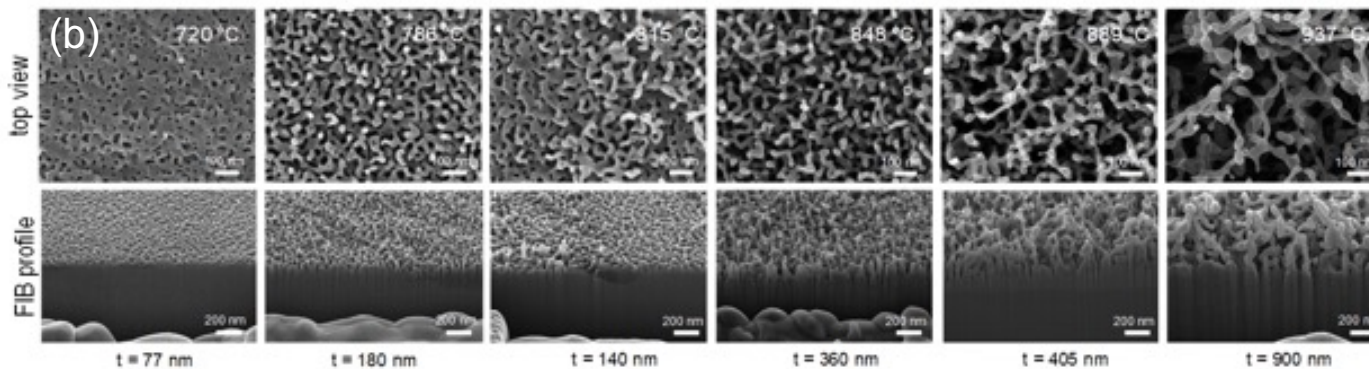
We used high temperature thermal desorption spectroscopy (TDS), helium ion microscopy, and in-situ spectroscopic ellipsometry to probe how W nanostructure grows during He plasma exposure.

Significance and Impact

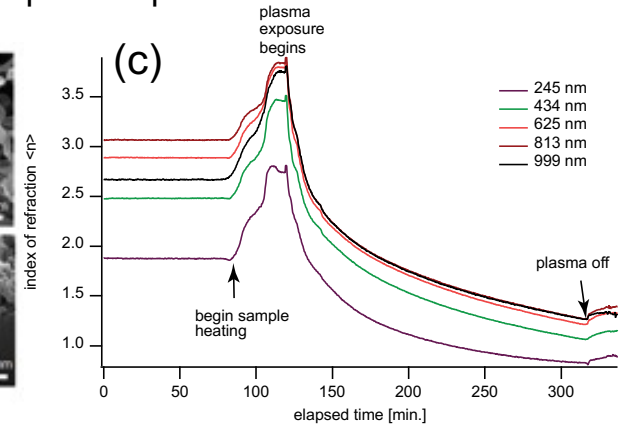
The in-situ ellipsometry provides a means of observing structural changes to the near-surface in real-time. These results complement ongoing modeling efforts by the University of Tennessee-led PMI SciDAC program.

Research Details

We exposed tungsten surfaces to RF-generated plasmas (exposure conditions: $\Gamma_{ion} = 8.5 \times 10^{20} \text{ m}^{-2} \text{ s}^{-1}$; $F = 7.9 \times 10^{23} - 3.6 \times 10^{25} \text{ m}^{-2}$, $T_{sample} = 450-930 \text{ }^\circ \text{C}$.) Helium ion microscopy was then used to image the initial surface morphology changes and nano-tendrils growth, c.f. Fig. (b). We correlated the microscopy data with the surface optical properties measured by an in-situ, real-time spectroscopic ellipsometry system. We observed a continuous decrease in both the extinction coefficient and index of refraction as a function of fluence between wavelengths of 280-1000 nm. The trapped He was measured via high-temperature TDS up to temperatures of 1600 °C.



He ion microscopy



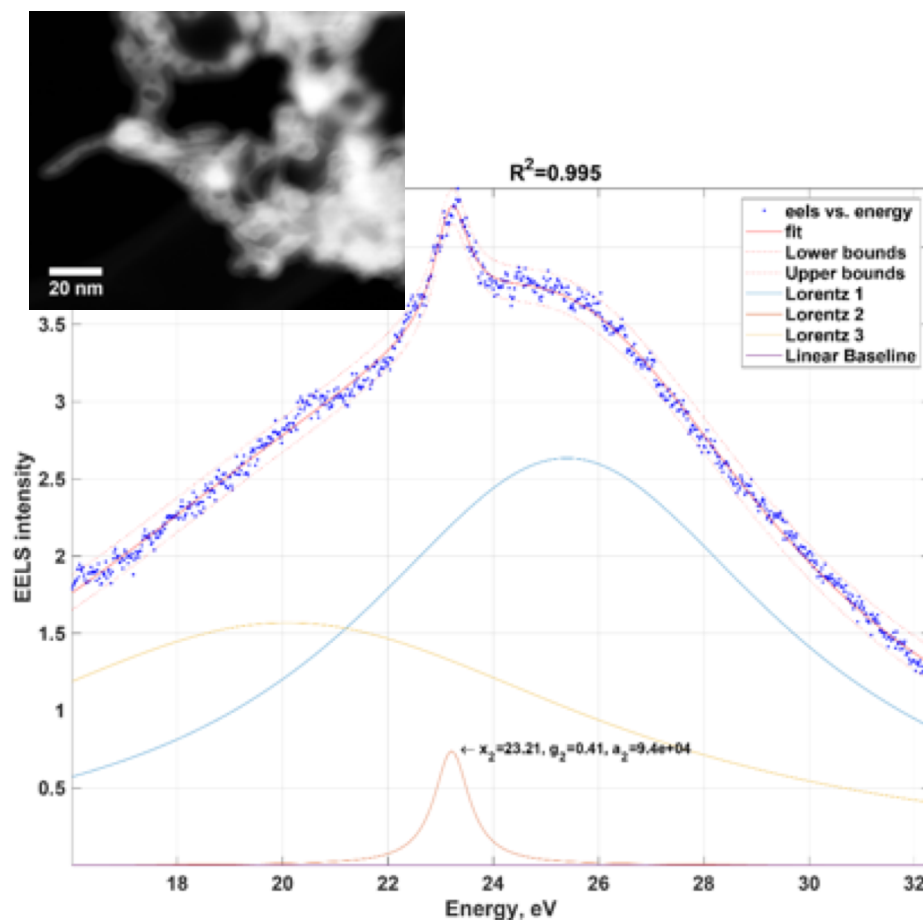
in-situ ellipsometry

A New Technique Will Allow the Measurement of Helium Pressure in Nanocavities

We need to know the pressure inside helium bubbles in PMI

- The pressure of helium bubbles in plasma-facing materials is an important parameter to understand and model in-service microstructure evolution
- **Monochromated, aberration-corrected electron microscopy can directly probe the helium state**
- Use of the ORNL MACSTEM (monochromated, aberration-corrected STEM) allowed unprecedented resolution in examining helium in tungsten nanotendrils.
- The tungsten plasmon (~ 25 eV) and surface plasmon (~ 18 eV) interfere with the He transition (21-25 eV), making monochromation necessary.
- We are presently analyzing data from ~ 50 bubbles to determine pressure vs. radius relationships.

Chad Parish, Kun Wang, Xunxiang Hu, Donovan Leonard (ORNL)
Russell Doerner, Matthew Baldwin (UCSD)



Monochromated EELS data showing a sharp helium transition on the background of the tungsten surface+bulk plasmons. The 21.2 eV free-atom transition has shifted to ~ 23.2 eV due to high pressure. (Estimated 1-5 GPa; refinements are underway.)
Inset: typical STEM image of nanofuzz containing bubbles.

Modeling the Effects of Helium Bubbles on the Stress-Strain Behavior of Iron Polycrystals

Science Objective

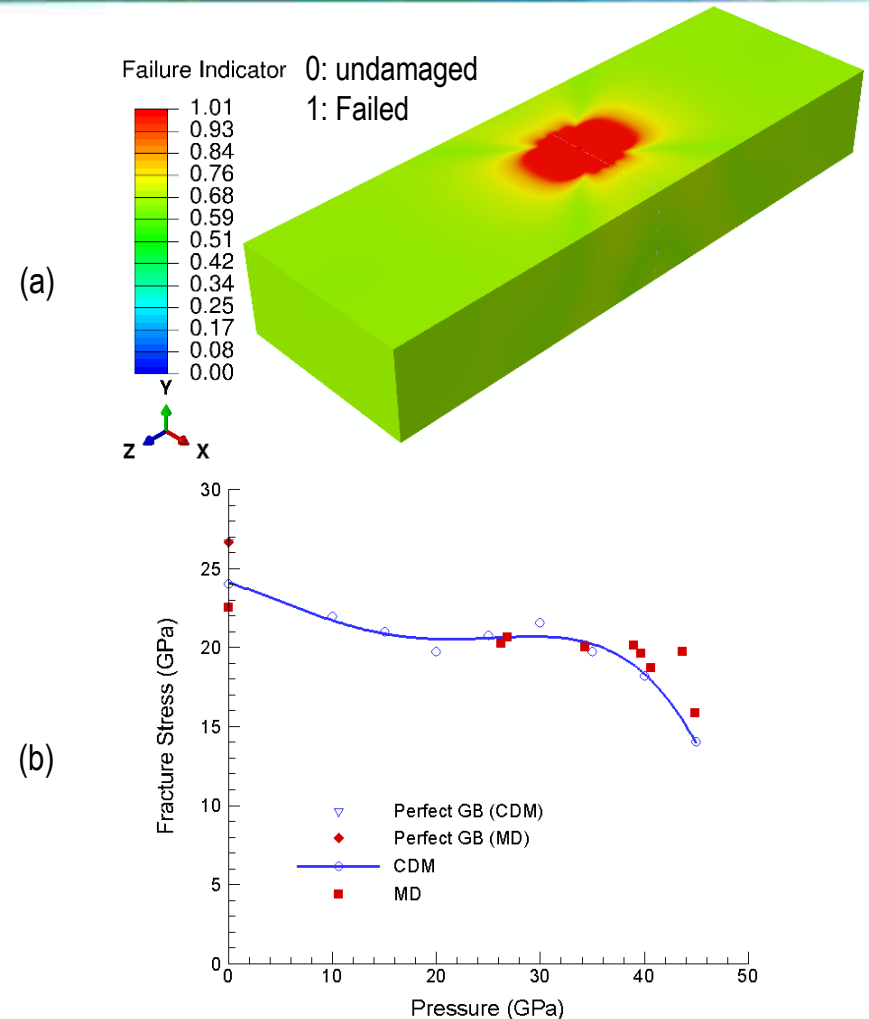
Investigate the effects of helium (He) bubbles on the stress-strain behavior of iron (Fe) polycrystals by a mechanistic finite element (FE) approach using a continuum damage mechanics (CDM) description of the material behavior informed by molecular dynamics (MD) data

Significance and Impact

Ferritic/martensitic steels experience He generation due to nuclear transmutation. This is a concern because He can cause hardening and embrittlement, swelling as a result of nucleation and growth of He bubbles, and reduced creep-rupture life. Since it is difficult to experimentally quantify the nano-scale effects of He bubbles, the MD-CDM approach developed very efficiently quantifies these effects on material integrity.

Research Details

MD tensile analyses of Fe single crystal and bicrystal are first performed to determine the crystal and perfect grain boundary (GB) behaviors. MD data are then used in 3D FE models of the homologue systems to identify the CDM and GB model parameters. Finally, FE analyses of the Fe bicrystal system subjected to uniaxial tension and He bubble pressure at the GB at low and room temperatures are conducted. CDM results are compared to the corresponding MD data for model validation.



Attractive retention properties in displacement damaged ultra-fine grain tungsten exposed to divertor plasma

Scientific Achievement

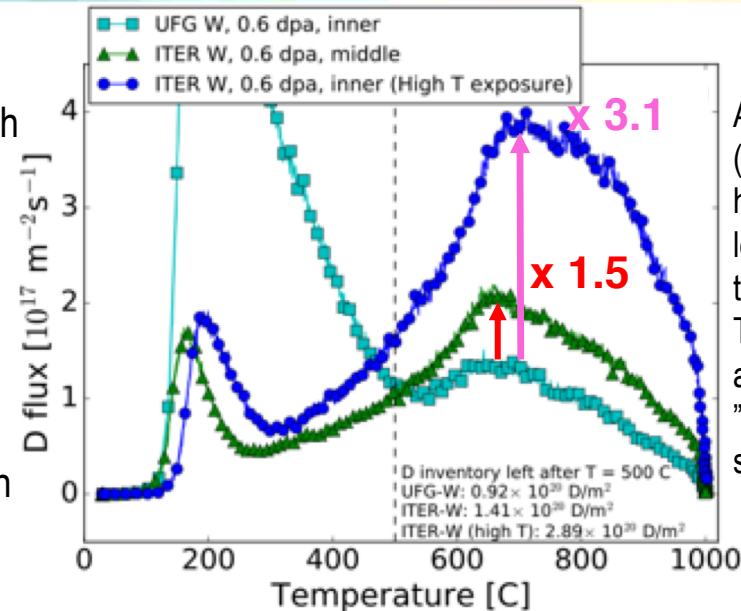
Ultra-fine grain tungsten (UFG W) retains less deuterium in high energy traps, compared to ITER-grade W, after undergoing lattice displacement damage.

Significance and Impact

Expected damage in the ITER W divertor is 0.6 displacements/atom (dpa) and requires $> 800^{\circ}\text{C}$ heating to remove trapped tritium. Most of the inventory in UFG W is removed with $< 500^{\circ}\text{C}$ heating (see top figure) so that retention of tritium in future reactors can be controlled with routine tile baking.

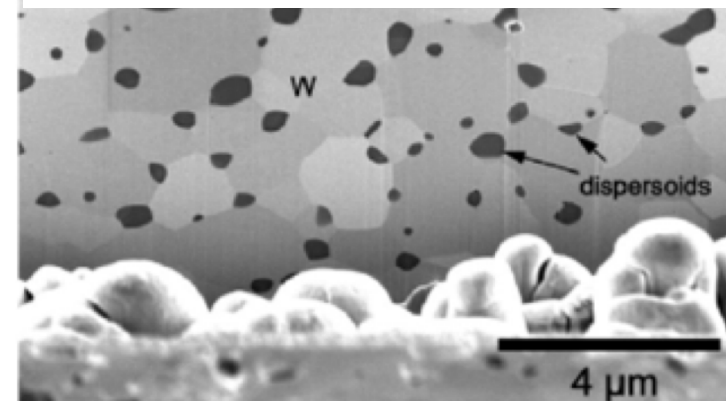
Research Details

UFG W (see lower figure) has small W grains with dispersoids that prevent recrystallization and should have improved resistance to radiation damage. ITER-grade and UFG W samples are damaged with 12 MeV Si ions then exposed to deuterium plasma in the DIII-D divertor. Retention is measured with $\text{D}(^3\text{He},p)\alpha$ NRA and then TDS. Modeling is underway to quantify trapping energies and diffusivity to better understand our observations.



After heating to 500°C (dashed line) UFG W has at least 1.5 times less trapped deuterium than ITER-grade W. The flux peaks $>500^{\circ}\text{C}$ are associated with "high energy" trap sites.

JL Barton, DA Buchenauer, WR Wampler, et al., (in preparation)
Nucl. Mater. & Energy (2018)



SEM image of a FIB cross-section of UFG W.

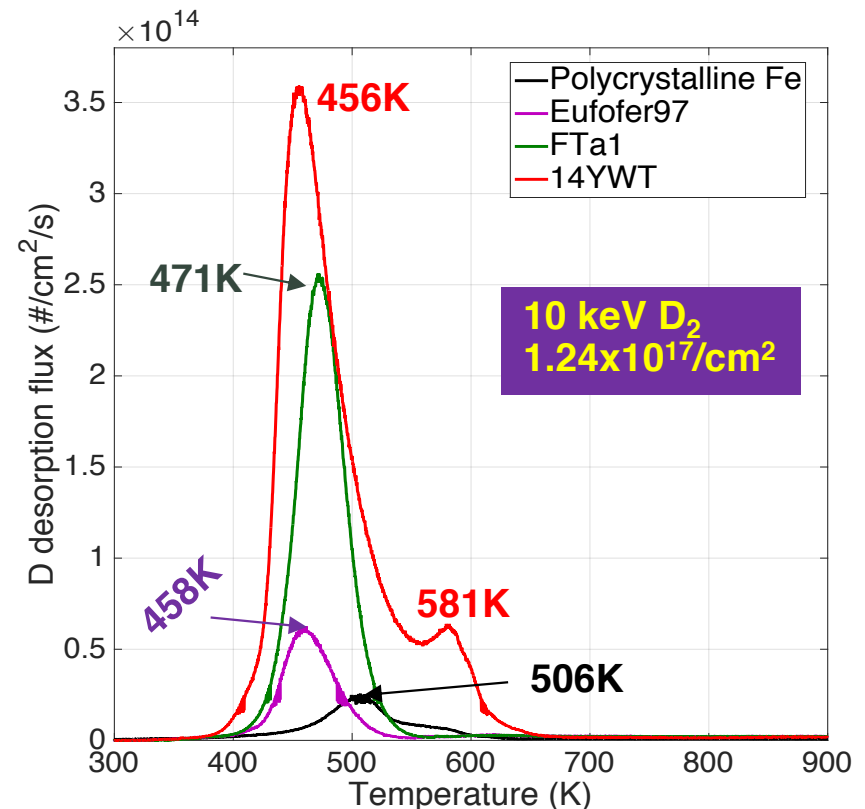
Kolasinski, et al., Int. J. Ref. Metals and Hard Mat. (2016)

Nanostructures in advanced fusion structural materials control deuterium retention

We investigated the deuterium trapping ability of nanostructures in advanced fusion reactor structural materials.

- Representative reduced activation ferritic-martensitic steels, castable nanostructure alloys, and oxide dispersion-strengthened alloys were selected for comparison of deuterium retention rate.
- Materials used were Eurofer 97 (RAFM), FTa1 (CNA) and 14YWT (ODS),
- Samples were implanted with 10 keV D₂ to 1.24x10¹⁷/cm² at room temperature.
- Thermal desorption measured D₂ release.
- The results showed that greater sink strength leads to more deuterium retention. The interface between nanoparticles (e.g., MX, M₂₃C₆, Y-Ti-O) and matrix serve as trapping sites (sinks) for deuterium.

Xunxiang Hu, Lizhen Tan, Sebastien N. Dryepondt, Caleb Massey, David T. Hoelzer, Yutai Katoh



Deuterium retention rate:

Fe: 5% Eurofer97: 9.9%

FTa1: 36.8% 14YWT: 47.3%

Deuterium desorption spectra from pure Fe and various advanced steels

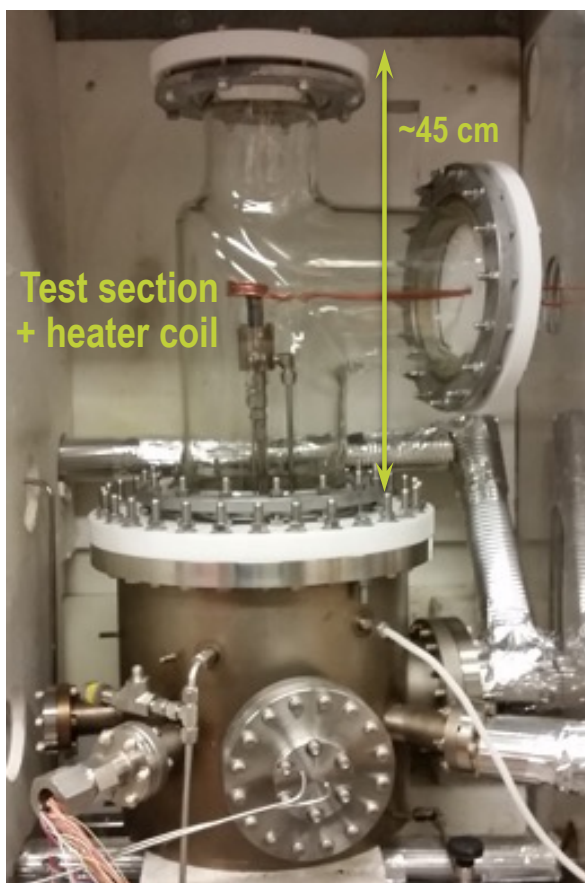
Thermal-Hydraulics Experiments on He-Cooled Solid Divertors

Application

Helium-cooled solid divertors leading candidate for solving power, particle exhaust issues in long-pulse fusion magnetic fusion devices

M. Yoda, S. I. Abdel-Khalik, S. A. Musa, D. S. Lee

Pyrex-stainless chamber



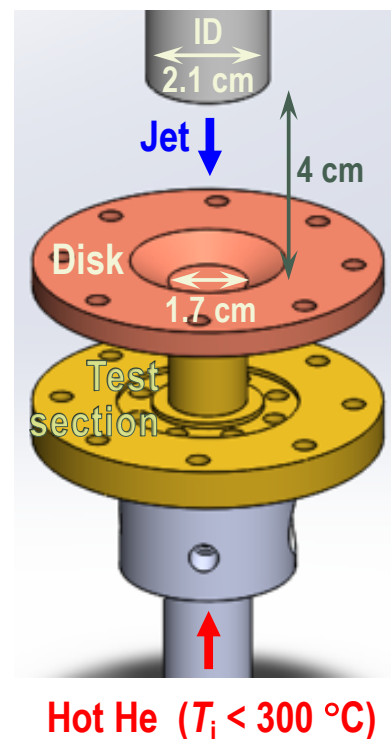
Research Details + Schedule

- Georgia Tech He loop upgrade
 - Modular finger divertor test section and RF heater coil enclosed in modified argon-filled Pyrex-stainless chamber to minimize W-alloy oxidation
 - Initial results: incident heat fluxes $q'' < 6.5 \text{ MW/m}^2$ at He inlet temperatures $T_i \approx 300 \text{ }^\circ\text{C}$
- Impinging (water) jet setup to evaluate reverse heat flux concept completed
 - Jet of ($20 \text{ }^\circ\text{C}$, 0.3 MPa) water at 5 kg/s impinges upon, and cools, copper disk heated by brass HEMJ test section in He loop
 - Updating numerical simulations to incorporate modifications to impinging jet setup
- Currently modifying He loop accommodate both reverse heat flux and divertor studies
 - Two abstracts submitted to TOFE23 (Orlando, FL)

Significance and Impact

Experimental studies of divertor thermal-hydraulics provide database for validating numerical simulations and a basis for future divertor concepts

Impinging jet setup



DAGMC Performance Improvements

Scientific Achievement

- Monte Carlo Radiation Transport (MCRT) performance competitive with analytic geometry used in native codes is demonstrated on tessellated CAD models of arbitrary complexity using DAGMC.

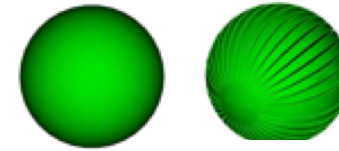
Significance and Impact

- DAGMC reduces human time required to create accurate models for MCRT by enabling the use of CAD tools for design iteration, but at the cost of additional computing time in simulation. This work aims to reduce simulation times on modern CPU architectures.

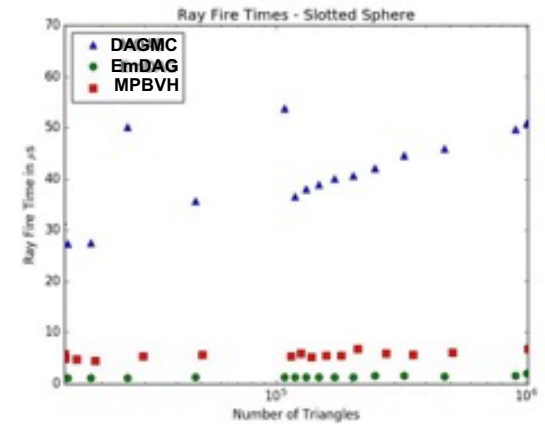
Research Details

- Intel's ray tracing kernel, Embree, was applied in an engineering analysis context (EmDAG), but found to be insufficient for robust particle tracking in an engineering context.
- Single precision traversal of spatial data structures are used to support double precision particle tracking for robust coupling to physics codes in a kernel dubbed the Mixed Precision Bounding Volume Hierarchy (MPBVH).
- Improvements in performance from 2 - 9.5x were observed in comparison to an unmodified version of DAGMC with no change in numerical results.

UW - Madison: P. Shriwise, A. Davis, P. Wilson; supported by NRC and DOE



DAGMC
EmDAG
MPBVH



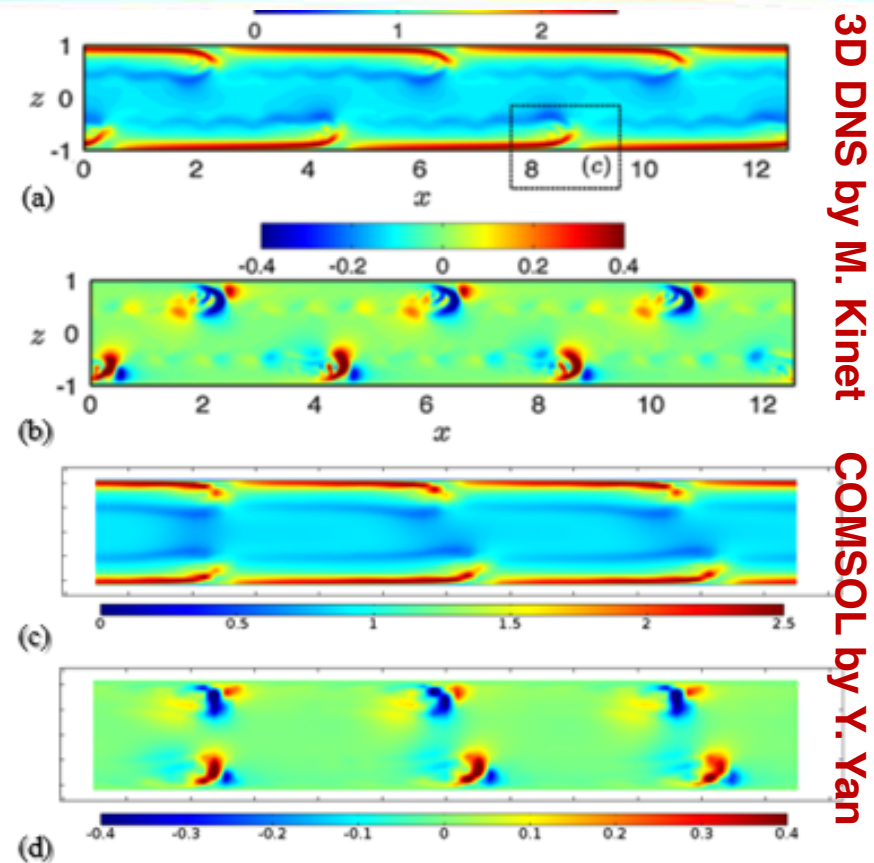
Ray tracing performance results

Model	Speedup Factor
Frascati Neutron Generator	2.09
Advanced Test Reactor	4.56
ITER-blite	9.54

Application to production simulations

Development of computational model for 3D MHD flows for fusion applications in COMSOL

- Use of commercial CFD software for computations of 3D LM MHD flows in fusion cooling applications is a relatively new but quickly growing effort [1]
- Of several CFD/MHD tools on the market (ANSYS CFX, FLUENT, COMSOL, STAR-CD), **COMSOL Multiphysics** is a very promising candidate
- **A computational model** for MHD duct flows has been established in COMSOL [2] and tested for all 5 benchmark cases proposed in [1]:
 - Fully developed MHD duct flows:** successful for Ha up to 15,000
 - 3D laminar developing MHD flows:** successful
 - Q2D MHD flow:** fair qualitative match
 - MHD turbulent flow:** fair qualitative match
 - MHD flow with heat transfer:** successful
- At present, we use COMSOL for the pre-experimental analysis of mixed-convection flows in MaPLE-U facility at UCLA
- ☐ Next effort – extending the COMSOL model to free-surface MHD flows and its application to LM PFC



3D DNS by M. Kinet
COMSOL by Y. Yan

Comparison between **COMSOL** (c and d) and **3D DNS** (a and b) in M. Kinet, et al., PRL, 2009 for turbulent MHD flow in a rectangular duct with thin electrically conducting walls at $Ha=200$, $Re=5000$.

[1] S. Smolentsev, et al., An approach to verification and validation of MHD codes for fusion applications, Fusion Eng. Des. 100, 65-72 (2015).

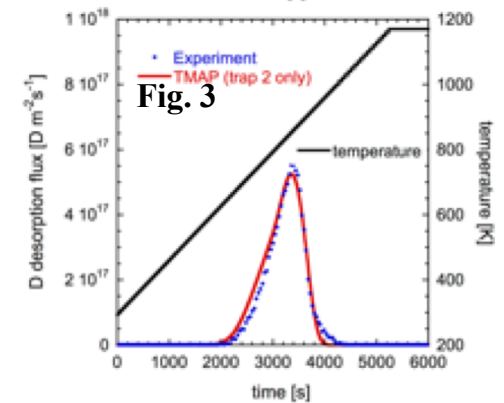
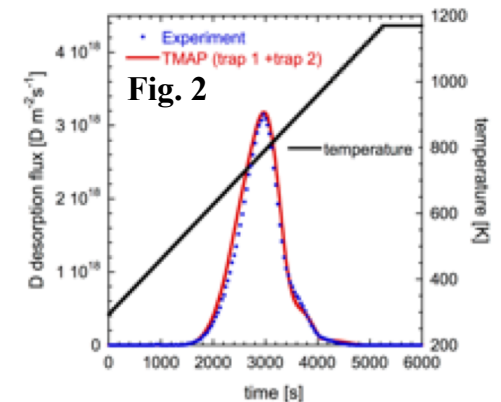
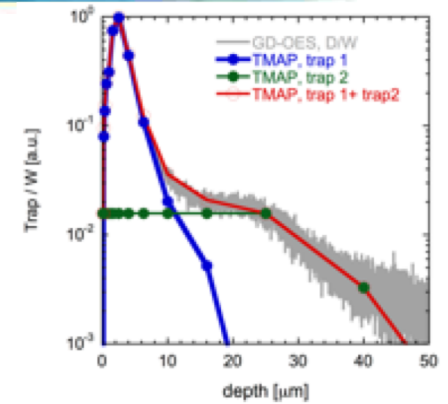
[2] Y. Yan, et al., Validation of COMSOL Multiphysics for magneto-hydro-dynamic (MHD) flows in fusion applications, COMSOL Conference, Boston, October 05 2017.

Improved Tritium Retention Modeling with Bulk Depth Profiling Capability

- Two critical challenges in understanding tritium retention modeling in PFCs is the unavailability of bulk deuterium (D) depth profiling beyond detection limit ($\sim 5\mu\text{m}$) of nuclear reaction analysis (NRA) and an incomplete understanding of defect trapping of the D.
- A glow-discharge optical emission spectroscopy (GD-OES) is a promising new diagnostic that is capable of providing bulk (up to $50\mu\text{m}$) D depth profiling [1-2].
- Two sets (A and B specimens) polycrystalline tungsten (W) specimens were exposed to identical D plasma conditions (100eV , $6.0 \times 10^{21} \text{ D/m}^2\text{-s}$, $5.0 \times 10^{25} \text{ D/m}^2$ with the Tritium Plasma Experiment (TPE). “A” specimens were used for thermal desorption study, and “B” specimens were used to obtain D depth profiling with GD-OES.
- A normalized GD-OES depth profile ($I_{D=121.534\text{nm}} / I_{W=429.461\text{nm}}$) was used as empty trap depth profile as shown in Fig.1.
- Initial results (Fig. 2 and 3) of D modeling in W with TMAP and bulk (up to $50 \mu\text{m}$) D depth profiling showed promising results [3].
- GD-OES will be used to provide bulk ($\gg 10\mu\text{m}$) D depth profiling from neutron-irradiated tungsten exposed to D plasma in FY19 Q4.

References

- [1] Y. Hatano, et al., Fus. Eng.. Des. 87 (2012) 1091,
 [2] C.N. Taylor and M. Shimada, AIP Advances 7 (2017) 055305
 [3] M. Shimada and C.N. Taylor, presented at 23rd PSI conference.



Tritium Processing Development for Magnetic Fusion

Application

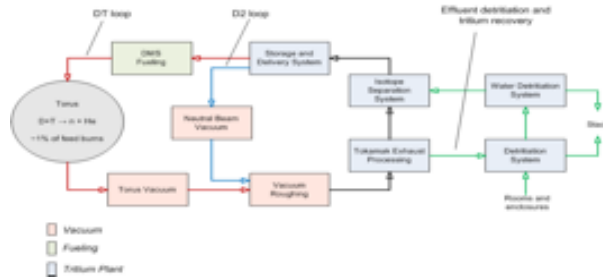
Development and testing of tritium fuel cycle components and data-mining of TSTA historical documentation.

Scientific Achievement

Heater controller, power supply and data acquisition system integrated into control panel.



Data Acquisition. Power Supply and Heater Controller Rack



ITER Fuel Cycle Block Diagram, example of typical needs for a fusion reactor fuel cycle system

Significance and Impact

- HPL and U-Bed upgrades will allow for continued engineering design development of tritium fuel cycle for fusion processes
- Integration of fuel cycle design into LM-PFC development will strengthen design options and applications.

Research Details

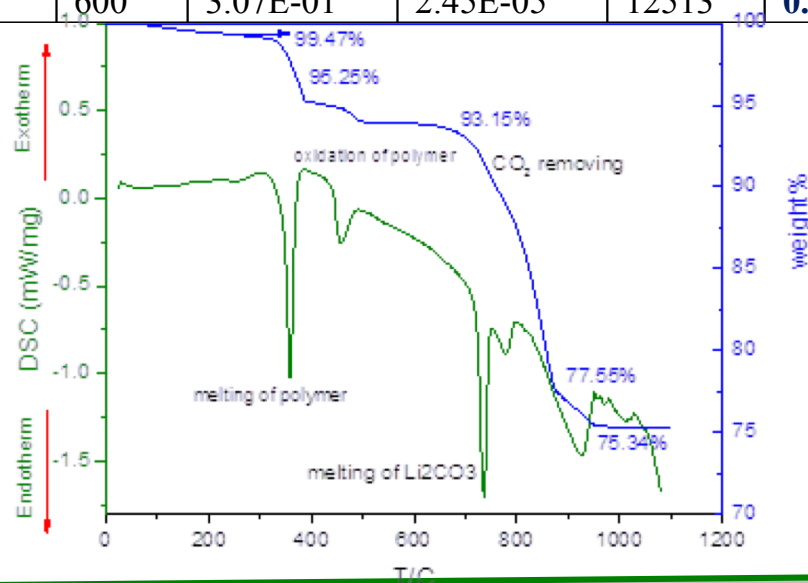
- Presented summary report at FNS Panel Review
- Presented Tritium Fuel Cycle Safety presentation at IAEA Workshop on Fusion Energy

Hollis, W. Kirk, LM PFC Meeting, Tritium Processing Development for Magnetic Fusion, Summary Report, April 2018

Hollis, W. Kirk, C. Taylor and S. Willms, Tritium Fuel Cycle Safety, IAEA Workshop on Fusion Energy, June 14th, 2018

Demonstration of Direct LiT Electrolysis using an Immersion Cell

Target	Temp (°C)	Ionic conductivity σ_i (S/cm)	Electrical conductivity σ_e (S/cm)	σ_i / σ_e	Ionic transference number τ
0.5B-LLZO	25	1.67E-05	-	-	-
	45	3.76E-05	2.71E-09	13875	0.9999
	110	4.06E-04	1.55E-07	2617	0.9996
	450	3.93E-02	1.33E-05	2945	0.9997
	600	7.13E-02	2.80E-05	2550	0.9996
0.5A-LLZO	21	7.58E-06	7.33E-10	10346	0.9999
	100	7.09E-04	2.89E-09	245294	1.0000
	450	2.26E-01	1.03E-05	21850	1.0000
	600	3.07E-01	2.45E-05	12513	0.9999



Scientific Achievement

- Developed a solution combustion synthesis method that can speed synthesis and lead to greater incorporation of lithium and other dopants while minimizing evaporation losses

Significance and Impact

- The development of a sol-gel or solution combustion synthesis allows significant variation of LLZO electrolyte properties and can be used to increase conductivity and strength of the electrolyte

Research Details

- Characterized both the electronic and ionic conductivity to understand the relative transport of electrons and ions
- Analysis showed that ionic transport in LLZO is greater than 3 orders of magnitude higher than electronic transport up to 600 °C
- Transference numbers near 1 confirm that LLZO electrolytes exceed the 0.0005 S/cm ionic conductivity target
- TGA/DSC was performed to understand critical temperatures during LLZO synthesis

Critical Issues for Liquid PFCs include Managing Power & Particle Fluxes and Shielding Vapor

Scientific Objective

Predict edge-plasma properties that are compatible with manageable heat flux and core plasma operation for FNSF design using liquid-metal walls. Compare results with similar configurations that used solid walls to identify key issues and impact on overall fusion performance.

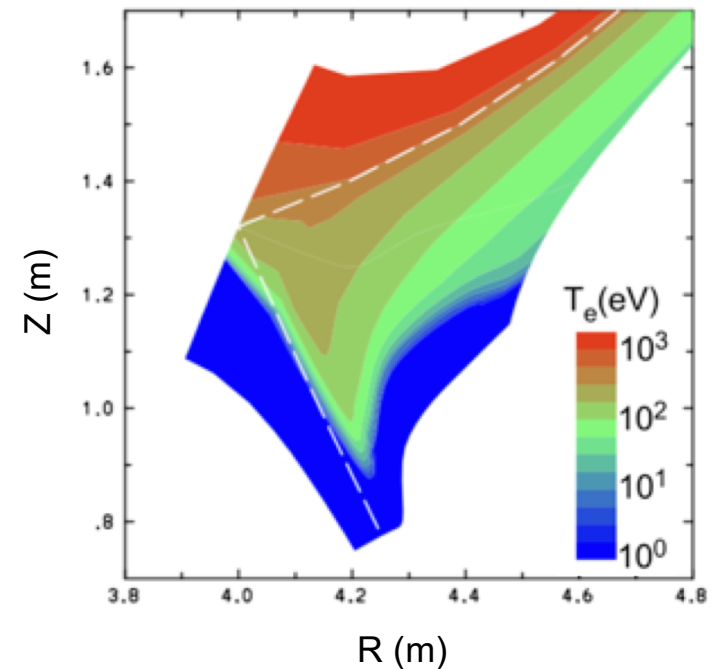
Achievement

Continued analysis of 2D UEDGE simulations for Li divertor in FNSF geometry to understand the impact of additional shaping of the divertor target plate. New simulations considered a slot-like divertor (right). Here a stable, fully detached divertor plasma is maintained with lithium injection from the private-flux wall and the divertor plate.

Why it matters

Flowing liquid walls could avoid the issue of wall erosion by ions and neutrals, and could also lead to high-performance core operational modes through high-temperature edge conditions.

Confinement of Li ions to the divertor is key to preventing lithium in the core region. A slot-like divertor design continues to yield a stable, detached divertor plasma.



Model edge plasmas for lithium-wall devices and power dropper operation to address key PFC issues

Scientific Objective

Develop and validate simulation model of hot kinetic ions striking PFCs in devices with Li walls. Also model dynamics of impurities from a particle dropper device and resulting wall-conditioning processes.

Achievement

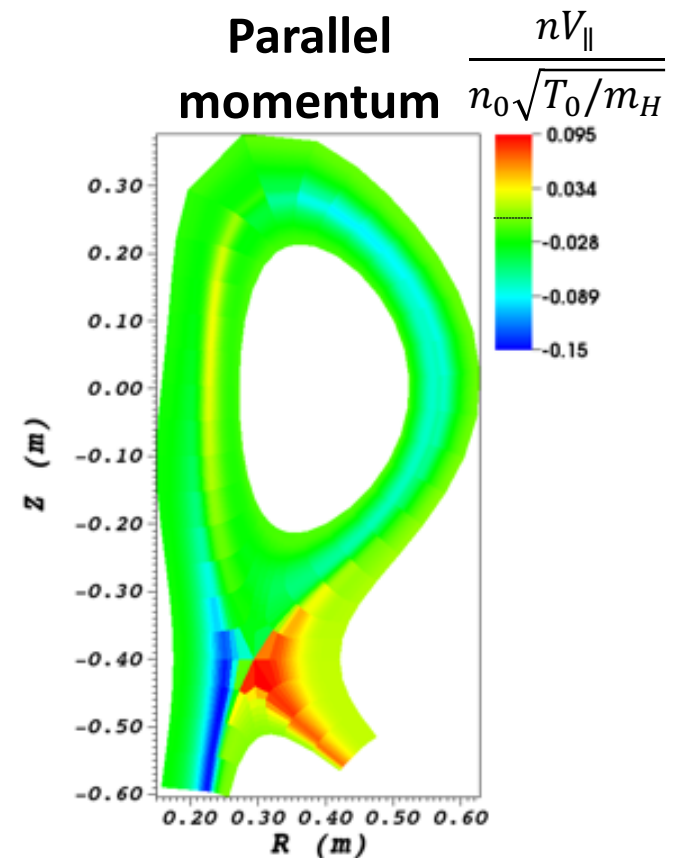
Extended 4D COGENT simulations of LTX kinetic ion distribution function including potential. Provides details of hot ion distribution function striking walls in low-recycling LTX. Plot illustrates strong B-field-induced ion flow variations.

A multi-institution workplan was developed at the PSI Conference to compare DIII-D power dropper data with modeling. Activities include experiments (PPPL), modeling powder ablation and ion deposition (LLNL & UCSD), and sheath/sputtering effects (UIUC).

Why it matters

Low-recycling devices with lithium PFCs such as LTX may provide greatly improved core energy confinement, but high edge temperatures can yield strong sputtering that must be evaluated. Wall conditioning by powder-dropping tools is a new, potentially revolutionary, techniques for real-time delivery of impurities into tokamak edge plasma; may allow real-time wall conditioning and advanced ways for maintaining radiative divertor

Ion flows to LTX divertor show strong kinetic effects



$$T_0 = 70 \text{ eV}$$